Article:

Yang, H., Ye, Y. and Chu, X. orcid.org/0000-0003-1863-6149 (2020) Max-min energy-efficient resource allocation for wireless powered backscatter networks. IEEE Wireless Communications Letters, 9 (5). pp. 688-692. ISSN 2162-2337

https://doi.org/10.1109/lwc.2020.2965942

Max-Min Energy-Efficient Resource Allocation for Wireless Powered Backscatter Networks

Haohang Yang, Yinghui Ye, Xiaoli Chu

***Abstract*—In this letter, we present the first attempt to solve an energy efficiency (EE) based max-min fairness problem for a wireless powered backscatter network where a power beacon (PB), which is a dedicated radio frequency (RF) power resource, and multiple backscatter devices work in the same frequency band. Each backscatter transmitter harvests energy from the signal transmitted by the PB, modulates its own information on the received signal, and backscatters the modulated signal to its associated receiver. We propose to ensure max-min fairness among the backscatter links by jointly optimizing the PB transmission power and the backscatter reflection coefficients. For analytical tractability, we solve the optimization problem for the case of two co-channel backscatter links by employing Lagrange dual decomposition when it is convex, and analyzing the monotonicity of the constraints when it is non-convex. Based on the obtained closed-form expressions of the optimal PB transmission power and the optimal backscatter reflection coefficients, we propose an iterative algorithm for max-min EE resource allocation. Simulation results show that the proposed iterative algorithm converges very fast and achieves a much fairer EE performance among backscatter links than maximizing the system EE of the network.**

***Index Terms*—Backscatter communications, energy efficiency, energy harvesting, max-min fairness.**

I. Introduction

Wireless powered backscatter communication has been considered as a promising technology to prolong the network lifetime of Internet of Things (IoT) systems [1]. In recent years, throughput maximization [2], signal detection [3] and hardware implementation [4] have been investigated for wireless powered backscatter communications, but the energy efficiency (EE) problem has not been sufficiently studied. The authors in [5] maximized the EE of a backscatter link by jointly optimizing the reflection coefficient and the power beacon (PB) transmission power. The EE maximization problem was studied for radio frequency (RF) powered cognitive backscatter communications [6]. However, both [5] and [6] considered only a single backscatter link and their results cannot be readily applied to multiple co-channel wireless powered backscatter links. Moreover, when multiple backscatter transmitters share the transmission power from a PB, it is necessary to ensure the fairness among the co-channel backscatter links.

In this letter, we consider a wireless powered backscatter network, where a PB and multiple backscatter links work in the same frequency band, and propose to maximize the minimum link EE among all the wireless powered backscatter links by jointly optimizing the PB transmission power and the backscatter reflection coefficients. The mutual interference between the multiple co-channel backscatter links and the interference from the PB to the backscatter receivers leads to complicated coupling effects between the backscatter reflection coefficients and the PB transmission power, resulting in a much higher complexity than that of EE maximization for one single backscatter link. As the complexity of the max-min EE problem increases with the number of co-channel links, and allowing more backscatter links to access the same channel may cause severe co-channel interference and increase the system complexity, which should be avoided because backscatter circuitry design needs to be kept simple [1]. For analytical tractability, we solve the problem for the case of two co-channel backscatter links. At the end, we obtain closed-form expressions for the optimal PB transmission power and the backscatter reflection coefficients. More specifically, the max-min EE problem is decomposed into two sub-problems conditioned on the convexity of the objective function: one is a convex optimization problem, while the other is non-convex. The convex problem is solved by employing Lagrange dual decomposition and KKT conditions, and the non-convex problem is solved by exploiting the characteristics of the associated constraints. Considering the low complexity and low cost requirements of backscatter devices [1], based on the obtained optimal solution, we propose an iterative algorithm that allows each backscatter transmitter to independently make optimal resource allocation decisions that maximize their EE while guaranteeing the fairness among the backscatter links.

II. System Model

As illustrated in Fig.1, we consider a wireless powered backscatter network[1] with a PB and M co-channel backscatter links, which are denoted by the set $\hat{D} = \{1, 2, \cdots, i, \cdots, M\}$. Backscatter link i consists of one backscatter transmitter i and one receiver i. Each node is equipped with a single antenna. We assume the availability of perfect channel state information (CSI) at each backscatter node [5]. In each time block T, the PB broadcasts a RF signal while each backscatter transmitter harvests energy from the received RF signal to support its circuit operation and modulates and reflects the received RF signal to carry its information to the associated receiver by properly setting a reflection coefficient.

Haohang Yang and Xiaoli Chu are with the Department of Electronic and Electrical Engineering, University of Sheffield, Sheffield, S1 4ET, United Kingdom (e-mail: hyang42@sheffield.ac.uk, x.chu@sheffield.ac.uk). The corresponding author is Dr. X. Chu.

Yinghui Ye is with the State Key Laboratory of Integrated Service Networks, Xidian University, Xi'an, 710071, China (e-mail: connectyyh@126.com).

[1]Note that different from the energy harvesting sensor or relay nodes in wireless powered communication networks (WPCN) or simultaneous wireless information and power transfer (SWIPT) networks that can set their own transmission power levels, the backscatter nodes directly modulate and reflect the incident RF signals transmitted by the PB. Furthermore, multiple variables including the PB transmission power and the reflection coefficients of co-channel backscatter links need to be jointly optimized in backscatter networks, while in WPCN or SWIPT networks, only the transmission power and the transmission time duration or power splitting ratio of sensor or relay nodes are optimized [7], [8].

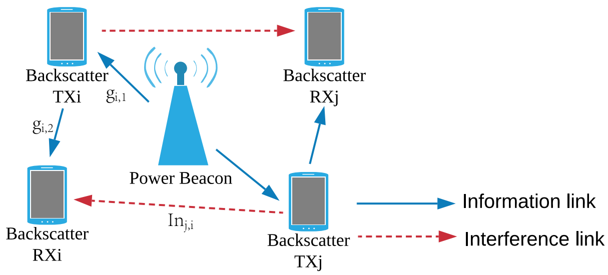

Fig. 1: Wireless powered backscatter networks.

In addition to the information carrying signal from backscatter transmitter i, receiver i also receives the co-channel interference from the other backscatter transmitters and the PB, and the received power at receiver i is given by $P_a g_{i,1} Z_i g_{i,2} + P_a g_{i,3} + \sum_{j=1,j\neq i}^{M} P_a g_{j,1} Z_j In_{j,i} + N_0$, where P_a is the transmission power of the PB; $Z_i \in$ [0,1], is the reflection coefficient of backscatter transmitter i and N_0 represents the additive white Gaussian noise (AWGN) power[2]; $g_{i,1}$ and $g_{i,2}$ denote the channel power gains from the PB to transmitter i and from backscatter transmitter i to receiver i, respectively; $In_{j,i}$ represents the channel power gain from backscatter transmitter j to receiver i, and $g_{i,3}$ denotes the channel power gain from the PB to receiver i. Since the PB serves as a RF energy source only, the transmitted signal from the PB is predefined and is known by all the backscatter receivers, thus receiver i can remove the interference from the PB, i.e., $P_a g_{i,3}$ [5]. Accordingly, the SINR at receiver i is written as

$$\mathrm{SINR}_i = \frac{P_a g_{i,1} Z_i g_{i,2}}{N_0 + \sum_{j=1,j\neq i}^{M} P_a g_{j,1} Z_j In_{j,i}}. \tag{1}$$

The throughput (bits/s) of backscatter link i is given by

$$R_i = T\log_2(1 + \mathrm{SINR}_i). \tag{2}$$

The energy harvested by backscatter transmitter i is

$$EH_i = P_a g_{i,1}(1 - Z_i)\eta T, \tag{3}$$

where $\eta \in$[0,1] is the energy conversion efficiency, for simplicity, the time block T is normalized to one, and we ignore the energy harvested from the thermal noise since it is very small [2], [5]. The backscatter transmitters are batteryless and cannot store the harvested energy. We assume that the energy harvested by transmitter i is used only for and is sufficient to support its circuit operation [5], i.e., $EH_i \geq PC_t$, where PC_t denotes the transmitter circuit power consumption and is assumed to be the same for all backscatter transmitters.

The power consumption for link i is composed of the RF transmission power P_a of the PB (which covers the backscatter transmitter circuit power consumption), and the total circuit power consumption at the PB and at receiver i, which is denoted by PC_r and is assumed to be the same for all receivers. Thus, the EE of backscatter link i is given by

$$EE_i = \frac{R_i}{P_a + PC_r}. \tag{4}$$

III. Max-Min EE Resource Allocation

A. Problem Formulation

We propose to maximize the minimum link EE among all co-channel backscatter links in order to improve the EE of the backscatter network while guaranteeing fairness among co-channel backscatter links. Accordingly, the optimization problem is formulated as

$$\begin{aligned} \mathbf{P1}: &\max_{\{P_a, Z_i\}} \min_{\{i\in\hat{D}\}} EE_i \\ \text{s.t. } &\mathrm{C1}: 0 < P_a \leq P_{\max}, \\ &\mathrm{C2}: 0 \leq Z_i \leq 1, i \in \hat{D}, \\ &\mathrm{C3}: R_i \geq R_{\min}, i \in \hat{D}, \\ &\mathrm{C4}: EH_i \geq PC_t, i \in \hat{D}, \end{aligned} \tag{5}$$

where C1 sets the maximum allowed transmission power P_{max} for the PB transmission power P_a; C2 sets the range of backscatter reflection coefficients; C3 sets the minimum throughput requirement $R_{\min}$ for backscatter links; and C4 ensures that the harvested energy of a backscatter transmitter is sufficient to cover its circuit power consumption. **P1** is a non-convex fractional optimization problem and is mathematically difficult to solve due to the coupling between variables P_a and Z_i in (1), (3), and (4).

From (1)−(4) we can see that EE_i increases with Z_i, while EH_i decreases with Z_i. Thus, the maximum EE_i is achieved when $EH_i = PC_t$. By solving $P_a g_{i,1}(1 - Z_i)\eta = PC_t$ for Z_i, we have

$$Z_i = 1 - \frac{PC_t}{P_a g_{i,1}\eta}. \tag{6}$$

By substituting (6) into (5), **P1** reduces to an optimization problem with respect to P_a only, which can be further transformed into a more tractable form following Lemma 1.

Lemma 1 [13]: After substituting (6) into (5), the optimal solution to **P1** can be obtained if and only if $\max_{\{P_a\}} \min_{\{i\in\hat{D}\}} R_i - Q^*(P_a + PC_r) = \min_{\{i\in\hat{D}\}} R_i{}^* - Q^*(P_a^* + PC_r) = 0$, where Q^* is the max-min EE, $R_i{}^*$ and P_a^* are the optimal throughput of backscatter link i and the optimal PB transmission power, respectively.

Based on (6) and Lemma 1, **P1** is converted to

$$\begin{aligned} \mathbf{P2}: &\max_{\{P_a\}} \min_{\{i\in\hat{D}\}} -Q(P_a + PC_r) + \\ &\log_2\left(1 + \frac{P_a g_{i,1} g_{i,2} - \frac{PC_t g_{i,2}}{\eta}}{P_a \sum_{j=1,j\neq i}^{M} g_{j,1} In_{j,i} - \sum_{j=1,j\neq i}^{M} \frac{PC_t In_{j,i}}{\eta} + N_0}\right) \\ &\text{s.t. C1, C5}: P_a \geq PC_t/g_{i,1}\eta, i \in \hat{D}, \\ &\mathrm{C6}: \\ &\log_2\left(1 + \frac{P_a g_{i,1} g_{i,2} - \frac{PC_t g_{i,2}}{\eta}}{P_a \sum_{j=1,j\neq i}^{M} g_{j,1} In_{j,i} - \sum_{j=1,j\neq i}^{M} \frac{PC_t In_{j,i}}{\eta} + N_0}\right) \geq R_{\min}. \end{aligned}$$

By introducing a slack variable Y, **P2** can be expressed as

$$\begin{aligned} \mathbf{P3}: &\max_{\{P_a, Y\}} Y \\ \text{s.t. } &\mathrm{C1, C5, C6}, \end{aligned} \tag{7}$$

[2]As the backscatter modulation order increases, the backscattered signals approximately follow a Gaussian distribution [9]-[12].

$$\text{C7}: \log_2\left(1+\frac{P_a g_{i,1}g_{i,2}-\frac{PC_t g_{i,2}}{\eta}}{P_a\sum_{j=1,j\neq i}^{M} g_{j,1}In_{j,i}-\sum_{j=1,j\neq i}^{M}\frac{PC_t In_{j,i}}{\eta}+N_0}\right) -Q(P_a+PC_r)\geq Y, i\in\hat{D}.$$

B. Convexity Analysis of **P3**

For notational simplicity, we rewrite C7 as

$$f_i(x)=\log_2\left(1+\frac{A_i x-B_i}{C_i x-D_i}\right)-Q(x+PC_r)-Y\geq 0, i\in\hat{D}, \tag{8}$$

where $x=P_a$, $A_i=g_{i,1}g_{i,2}$, $B_i=\frac{PC_t g_{i,2}}{\eta}$, $C_i=\sum_{j=1,j\neq i}^{M} g_{j,1}In_{j,i}$, $D_i=\sum_{j=1,j\neq i}^{M}\frac{PC_t In_{j,i}}{\eta}-N_0$, and $A_i,B_i,C_i\geq 0$.

Taking the first-order derivative of $f_i(x)$ with respect to x, $i\in\hat{D}$ we obtain

$$f_i'(x)=\frac{(B_iC_i-A_iD_i)\log_2 e}{(C_ix-D_i+A_ix-B_i)(C_ix-D_i)}-Q. \tag{9}$$

The second-order derivative of $f_i(x)$ is obtained as

$$f_i''(x)=\frac{-(B_iC_i-A_iD_i)\log_2 e}{(C_ix-D_i+A_ix-B_i)(C_ix-D_i)} \times\frac{(C_i+A_i)(C_ix-D_i)+(C_ix-D_i+A_ix-B_i)C_i}{(C_ix-D_i+A_ix-B_i)(C_ix-D_i)}. \tag{10}$$

Based on (6) and C2, $i\in\hat{D}$, we have $A_ix-B_i\geq 0$ and $C_ix-D_i\geq 0$. If $B_iC_i-A_iD_i>0$, then $f_i''(x)<0$ and **P3** is convex; otherwise, $f_i''(x)\geq 0$ and **P3** is non-convex. We will solve **P3** for these two cases, respectively. However, **P3** is still intractable mainly due to the complexity of C7, which increases with M. In the following, we will solve **P3** for the case of $M=2$, i.e., when there are two co-channel backscatter links in the network.

C. Solution of Convex **P3**

When $B_iC_i-A_iD_i>0$ for $i\in\{1,2\}$, **P3** is a convex problem with respect to P_a and Y. By employing Lagrange dual decomposition, we obtain

$$L(x,Y,\alpha,\beta_i,\theta_i,\phi_i)=\alpha\left(P_{max}-x\right)+\sum_{i=1}^{2}\beta_i\left(x-\frac{PC_t}{g_{i,1}}\right) +\sum_{i=1}^{2}\theta_i\left[\log_2\left(1+\frac{A_ix-B_i}{C_ix-D_i}\right)-R_{\min}\right]+Y +\sum_{i=1}^{2}\phi_i\left[\log_2\left(1+\frac{A_ix-B_i}{C_ix-D_i}\right)-Q(x+PC_r)-Y\right], \tag{11}$$

where $\alpha,\beta_i,\theta_i,\phi_i$ are the Lagrange multipliers associated with the constraints of **P3**.

To solve $\frac{\partial L(x,Y,\alpha,\beta_i,\theta_i,\phi_i)}{\partial x}=0$, we rewrite it as

$$k_1x^4+k_2x^3+k_3x^2+k_4x+k_5=0, \tag{12}$$

where $k_1=Ja_1a_2, k_2=-J(b_1a_2+a_1b_2), k_3=JC_1a_2+Jb_1b_2+Ja_1C_2-Ea_2-Fa_1, k_4=Eb_2+Fb_1-JC_1b_2-Jb_1C_2, k_5=Jc_1c_2-Ec_2-Fc_1, a_1=C_1^2+A_1C_1, b_1=2C_1D_1+B_1C_1+A_1D_1, c_1=B_1D_1+D_1^2, a_2=C_2^2+A_2C_2, b_2=2C_2D_2+B_2C_2+A_2D_2, c_2=B_2D_2+D_2^2, E=(\theta_1+\phi_1)(B_1C_1-A_1D_1), F=(\theta_2+\phi_2)(B_2C_2-A_2D_2), J=(\alpha-(\beta_1+\beta_2)+2Q)\ln 2$.

Then we obtain the four roots of (12) as [14]

$$x_{1,2}=\left[-\frac{k_2}{4k_1}-S\pm\frac{\sqrt{-4S^2-2p+\frac{q}{s}}}{2}\right]^+, \tag{13}$$

$$x_{3,4}=\left[-\frac{k_2}{4k_1}+S\pm\frac{\sqrt{-4S^2-2p-\frac{q}{s}}}{2}\right]^+, \tag{14}$$

where $[X]^+=\max(0,X), p=\frac{8k_1k_3-3k_2^2}{8k_1^2}, q=\frac{k_2^3-4k_1k_2k_3+8k_1^2k_4}{8k_1^3}, S=\frac{1}{2}\sqrt{-\frac{2}{3}p+\frac{T+\frac{\Delta_0}{T}}{3k_1}}, T=\sqrt[3]{\frac{\Delta_1+\sqrt{\Delta_1^2-4\Delta_0^3}}{2}}, \Delta_1=2k_3^3-9k_2k_3k_4+27k_2^2k5+27k_1k_4^2-72k_1k_3k_5$, and $\Delta_0=k_3^2-3k_2k_4+12k_1k_5$.

For any given Y, the optimal value of P_a is given by

$$P_a^*=\max(x_1,x_2,x_3,x_4). \tag{15}$$

Substituting (15) into (7), we can calculate Y^* as

$$Y^*=\min_{\{i\in\hat{D}\}}\left(\log_2\left(1+\frac{A_iP_a^*-B_i}{C_iP_a^*-D_i}\right)-Q\left(P_a^*+PC_r\right)\right). \tag{16}$$

The Lagrange multipliers are updated by using the subgradient method [15].

D. Solution of Non-convex **P3**

If $B_iC_i-A_iD_i\leq 0$ for $i\in\hat{D}$, then C7 is non-convex and **P3** cannot be solved using convex optimization methods. In the following, we analyze the monotonicity of C7 to solve **P3**. Based on (8), $B_iC_i-A_iD_i$, $i\in\{1,2\}$ can be written as

$$B_1C_1-A_1D_1=\frac{PC_tg_{1,2}}{\eta}In_{2,1}(g_{2,1}-g_{1,1})+g_{1,1}g_{1,2}N_0, \tag{17}$$

$$B_2C_2-A_2D_2=\frac{PC_tg_{2,2}}{\eta}In_{1,2}(g_{1,1}-g_{2,1})+g_{2,1}g_{2,2}N_0. \tag{18}$$

From (17) and (18), we can see that if $g_{2,1}-g_{1,1}>0$, then $B_1C_1-A_1D_1>0$ and $B_2C_2-A_2D_2\leq 0$, leading to $f_1''(x)<0$ and $f_2''(x)\geq 0$; Otherwise, $B_1C_1-A_1D_1\leq 0$ and $B_2C_2-A_2D_2>0$, leading to $f_1''(x)\geq 0$ and $f_2''(x)<0$.

Without loss of generality, in the following, we assume $B_1C_1-A_1D_1\leq 0$, thus $f_1''(x)\geq 0$ and $f_2''(x)<0$. Based on (8)–(10), we can see that $f_1(x)$ is a monotonically decreasing function of x and $f_2(x)$ is a concave function of x while meeting all the constraints of **P3**. The relationship between $f_1(x)$ and $f_2(x)$ can be analyzed by defining

$$h(x)=f_1(x)-f_2(x)=\log_2\left(1+\frac{A_1x-B_1}{C_1x-D_1}\right) -\log_2\left(1+\frac{A_2x-B_2}{C_2x-D_2}\right), \tag{19}$$

and calculating

$$h'(x)=\frac{(B_1C_1-A_1D_1)\log_2 e}{(C_1x-D_1+A_1x-B_1)(C_1x-D_1)} -\frac{(B_2C_2-A_2D_2)\log_2 e}{(C_2x-D_2+A_2x-B_2)(C_2x-D_2)}. \tag{20}$$

Since $B_1C_1-A_1D_1\leq 0$, we have $h'(x)\leq 0$, indicating that there is at most one intersection between $f_1(x)$ and $f_2(x)$.

Then we need to find the range of x. Denoting the feasible value range for x by $[x_{min}, x_{max}]$, based on C1, C5 and C6, we obtain that

$$x_{min} = \max\left(\frac{B_i - D_i(2^{R_{\min}} - 1)}{A_i - C_i(2^{R_{\min}} - 1)}, \frac{PC_t}{g_{i,1}\eta}\right), i \in \{1, 2\}, \tag{21}$$

$$x_{max} = P_{\max}. \tag{22}$$

Based on the above analysis, we can solve non-convex **P3** under the following 2 conditions.

Condition 1. $h(x_{min})h(x_{max}) > 0$: $f_1(x)$ and $f_2(x)$ do not intersect, and the maximum value of Y is given by

$$Y^* = \min(\max_{\{x\}} f_1(x), \max_{\{x\}} f_2(x)). \tag{23}$$

Since $f_1(x)$ is a monotonically decreasing function of x, $\max_{\{x\}} f_1(x) = f_1(x_{min})$, and $x_1^* = x_{min}$. Since $f_2(x)$ is a concave function, to obtain $x_2^* = \arg\max_{\{x\}} f_2(x)$, we solve $f_2'(x) = 0$ for x and get

$$G = \frac{-u_2 \pm \sqrt{u_2^2 - 4u_1u_3}}{2u_1}, G \in [x_{min}, x_{max}], \tag{24}$$

where $u_1 = (C_2^2 + A_2C_2)$, $u_2 = -(2C_2D_2 + B_2C_2 + A_2D_2)$ and $u_3 = D_2^2 + B_2D_2 - \frac{\log_2 e(B_2C_2 - A_2D_2)}{Q}$. Then we have

$$x_2^* = \begin{cases} x_{max}, & G \geq x_{max}, \\ G, & x_{min} < G < x_{max}, \\ x_{min}, & G \leq x_{min}. \end{cases} \tag{25}$$

Therefore, the optimal value of x is given by

$$x^* = \arg\min_{x_1^*, x_2^*}(f_1(x_1^*), f_2(x_2^*)). \tag{26}$$

Condition 2. $h(x_{min})h(x_{max}) \leq 0$: $f_1(x)$ and $f_2(x)$ have one intersection, which can be further divided into the following three cases.

Case (i). If $f_2'(x_{min}) \leq 0$, then $f_2'(x) < 0, x \in [x_{min}, x_{max}]$. In this case, $f_1(x)$ and $f_2(x)$ are both monotonically decreasing functions of x, and we obtain

$$x^* = x_{min}. \tag{27}$$

Case (ii). If $f_2'(x_{max}) \geq 0$, then $f_2'(x) > 0, x \in [x_{min}, x_{max}]$. In this case, $f_2(x)$ is a monotonically increasing function of x, and the optimal x occurs at the intersection. Solving $f_1(x) = f_2(x)$ for x, we obtain

$$x^* = H = \frac{-n_2 \pm \sqrt{n_2^2 - 4n_1n_3}}{2n_1}, x \in [x_{min}, x_{max}], \tag{28}$$

where $n_1 = A_1C_2 - C_1A_2$, $n_2 = D_1A_2 + C_1B_2 - B_1C_2 - A_1D_2$, $n_3 = B_1D_2 - B_2D_1$, and H denotes the intersection value of x.

Case (iii). If $f_2'(x_{min}) > 0$ and $f_2'(x_{max}) < 0$, then $f_2(x)$ first increases and then decreases with x in $[x_{min}, x_{max}]$, and we obtain

$$P_a{}^* = \begin{cases} G, & f_1(x_{min}) > f_2(x_{min}) \;\&\; f_1(G) \geq f_2(G), \\ H, & f_1(x_{min}) > f_2(x_{min}) \;\&\; f_1(G) \leq f_2(G), \\ x_{min}, & f_1(x_{min}) \leq f_2(x_{min}). \end{cases} \tag{29}$$

Based on the obtained solutions to convex **P3** and non-convex **P3**, we propose an iterative algorithm in Algorithm 1 to solve **P3** and obtain the global optimal values of P_a^* and Z_i^*. In Algorithm 1, t is the index of iteration of the main loop; I is the predefined maximum allowed number of iteration of the main loop, and ψ is a very small value set to check whether the objective function in **P3** converges.

Algorithm 1 Iterative algorithm

Input: $\hat{D} = \{1, 2\}$.
Output: P_a^*, Z_i^*.
Initialize: $Q(t) = Q(0), Y(t) = Y(0), I, \psi, t = 0$.

```
while t < I do
  if B_iC_i − A_iD_i > 0, i ∈ D̂ then
    for n = 1 to I_1 do
      for u = 1 to I_2 do
        We use Q_u(t) and Y_u(t) to obtain P_{a,u}(t+1) by calculating (15).
        We use obtained P_{a,u}(t+1) to calculate Y_u(t+1) by calculating (16).
      end for
      Q_u(t+1) = R_i P_{a,u}(t+1)/[P_{a,u}(t+1) + PC_r].
      We update Lagrange multipliers by using a sub-gradient method.
    end for
  else
    We obtain Y(t+1) and P_a(t+1) under Condition 1 or Condition 2.
    Q(t+1) = R_i P_a(t+1)/[P_a(t+1) + PC_r].
  end if
  if | min_{i∈D̂} R_i(P_a(t+1)) − Q(t+1)(P_a(t+1) + PC_r) | ≤ ψ then
    P_a^* = P_a(t+1), obtain Z_i^* using (6), obtain EE_1 and EE_2 using (4).
    Break
  end if
  t = t + 1.
end while
```

IV. Simulation Results

In this section, we present the simulation results to evaluate the performance of our proposed max-min EE resource allocation scheme in comparison with the criterion of maximizing system EE (max-SEE) under the case of two co-channel backscatter links. We consider distance dependent pathloss as large scale fading, where the pathloss exponent is set as 2.5, and rayleigh fading as small scale fading which follows a unit mean exponential distribution. The transmission radius of PB is set as 30 m; the distance between a backscatter transmitter and its receiver is denoted as r, which is less than 15 m for all backscatter links. P_{max}=23 dBm, N_0=−114 dBm, $\eta = 0.6$, PC_t=0.1 mw, PC_r=110 mw, R_{min}=3 bits/Hz.

Fig. 2 shows the convergence of the iterative algorithm for three cases with different distance (r) between a backscatter transmitter and its receiver. We can see that the max-min EE converges in the $4th \sim 6th$ iteration, and a higher EE is obtained for a smaller r. It is because the throughput increases

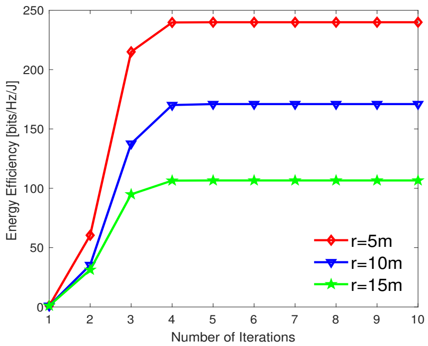

Fig. 2: Iterative algorithm for different value of *r*.

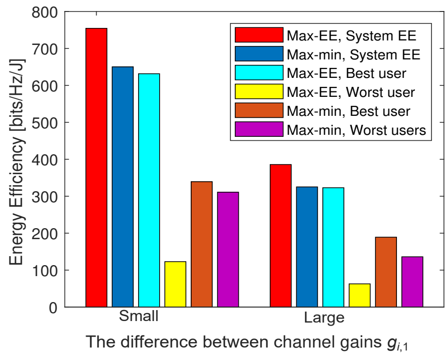

Fig. 3: EE versus channel power gain differences between $g_{i,1}$ and $g_{j,1}$.

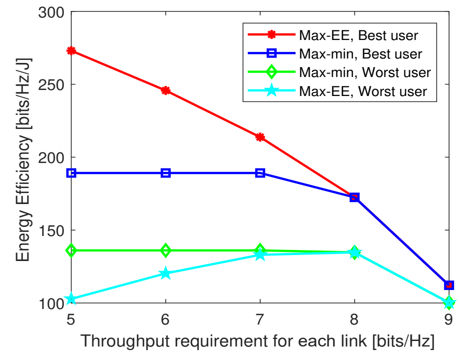

Fig. 4: EE versus throughput requirement for backscatter links.

for a shorter communication distance, leading to a higher EE. Fig. 2 proves that our proposed iterative algorithm is efficient to converge fast.

In Fig. 3, we compare the EE under max-min fairness and max-SEE versus the channel power gain differences between $g_{i,1}$ and $g_{j,1}$. On the one hand, we can see that the max-SEE algorithm achieves a higher system EE than our proposed Algorithm 1. However, the EE gap between the best user and the worst user is too large, which is significantly reduced by ensuring max-min fairness. On the other hand, in the first case, the EE of the worst user under the max-SEE criterion improves 31.53% by employing max-min fairness; while in the second case, the EE of the worst user improves 25.55%. This indicates that the max-min fairness is less effective when the channel power gain difference between $g_{i,1}$ and $g_{j,1}$ becomes larger. This is because when the channel power gain difference becomes larger, the EE difference between the best user and the worst user becomes larger so that it will be harder to achieve fairness. This also proves that the max-SEE algorithm tends to favour the best user.

Fig. 4 shows the EE versus the throughput requirement for backscatter links under the criterions of max-min fairness and max-SEE. A higher throughput requirement reduces the range of P_a, which may change the obtained optimal solution of P_a. Before the throughput requirement increases to 8 bits/Hz, based on the max-SEE, which tends to favour the best user, when the range of P_a reduces, the best user cannot obtain its optimal value of P_a which makes its EE lower. But the worst user forwards to its optimal value so that its EE improves. When we consider max-min fairness, EE of the best user and the worst user keeps unchanged and begins to drop after the throughput requirement greater than 7 bits/Hz, this is because that the obtained optimal solution of P_a first keeps unchanged and then changes for both the best user and the worst user. After the throughput requirement exceeds 8 bits/Hz, the EE of the best user and the worst user under both criterions reduces since both the users cannot obtain their optimal value of P_a. Also, the EE gap between the best user and the worst user becomes smaller, and the optimal solutions under the criterions of both max-min fairness and max-SEE are the same.

V. Conclusions

In this letter, we solve the max-min EE resource allocation problem in a wireless powered backscatter network. An iterative algorithms is proposed to solve this problem by jointly optimizing the transmission power of the PB and the reflection coefficients when the optimization problem is convex or non-convex. Simulation results show that the iterative algorithm converges very fast, and the max-min EE resource allocation is more effective when the throughput requirement is low and the channel power gain difference from the PB to each backscatter transmitter is small.

References

[1] N. Van Huynh, D. T. Hoang, X. Lu, D. Niyato, P. Wang and D. I. Kim, "Ambient Backscatter Communications: A Contemporary Survey," *IEEE Commun. Surv. Tutor.*, vol. 20, no. 4, pp. 2889-2922, Fourthquarter 2018.

[2] B. Lyu, C. You, Z. Yang and G. Gui, "The Optimal Control Policy for RF-Powered Backscatter Communication Networks," *IEEE Trans. Veh. Technol.*, vol. 67, no. 3, pp. 2804-2808, March 2018.

[3] Q. Zhang, H. Guo, Y. Liang and X. Yuan, "Constellation Learning-Based Signal Detection for Ambient Backscatter Communication Systems," *IEEE J. Sel. Areas Commun.,* vol. 37, no. 2, pp. 452-463, Feb. 2019.

[4] B. Kellogg et al., "Wi-Fi Backscatter: Internet Connectivity for Powered Devices," in *Proc. ACM SIGCOMM*, 2014, pp. 607-618.

[5] Y. Ye, L. Shi, R. Q. Hu and G. Lu, "Energy-Efficient Resource Allocation for Wirelessly Powered Backscatter Communications," *IEEE Commun Lett.*, vol. 23, no. 8, pp. 1418-1422, Aug. 2019.

[6] R. Kishore, S. Gurugopinath, P. C. Sofotasios, S. Muhaidat and N. Al-Dhahir, "Opportunistic Ambient Backscatter Communication in RF-Powered Cognitive Radio Networks," *IEEE Trans. Cogn. Commun. Netw.*, vol. 5, no. 2, pp. 413-426, June 2019.

[7] L. Xie, J. Xu and R. Zhang, "Throughput Maximization for UAV-Enabled Wireless Powered Communication Networks,"*IEEE Internet Things J.,* vol. 6, no. 2, pp. 1690-1703, April 2019.

[8] N. Zhao, R. Chai, Q. Hu and J. Zhang, "Energy Efficiency Optimization Based Joint Relay Selection and Resource Allocation for SWIPT Relay Networks", in *Proc. IEEE ChinaCom*, Shanghai, 2015, pp. 503-508.

[9] C. Boyer and S. Roy, "Backscatter Communication and RFID: Coding, Energy, and MIMO Analysis,"*IEEE Trans. Commun.*, vol. 62, no. 3, pp. 770785, Mar. 2014.

[10] R. Correia, A. Boaventura, and N. Borges Carvalho, "Quadrature Amplitude Backscatter Modulator for Passive Wireless Sensors in IoT Applications,"*IEEE Trans. Microw. Theory Tech.*, vol. 65, no. 4, pp. 11031110, Apr. 2017.

[11] W. Liu, K. Huang, X. Zhou and S. Durrani, "Full-Duplex Backscatter Interference Networks Based on Time-Hopping Spread Spectrum, "*IEEE Trans. Wireless Commun.*, vol. 16, no. 7, pp. 4361-4377, July 2017.

[12] W. Liu, Y. Liang, Y. Li and B. Vucetic, "Backscatter Multiplicative Multiple-Access Systems: Fundamental Limits and Practical Design,"*IEEE Trans. Wireless Commun.*, vol. 17, no. 9, pp. 5713-5728, Sept. 2018.

[13] W. Dinkelbach, "On Nonlinear Fractional Programming," *Manage. Sci.*, vol. 13, no. 7, pp. 492-498, Mar. 1967.

[14] Y. Ye et al., "Dynamic Asymmetric Power Splitting Scheme for SWIPT-Based Two-Way Multiplicative AF Relaying," *IEEE Signal Process. Lett.*, vol. 25, no. 7, pp. 1014-1018, July 2018.

[15] Wei Yu and R. Lui, "Dual methods for nonconvex spectrum optimization of multicarrier systems,"*IEEE Trans. Commun.,* vol. 54, no. 7, pp. 1310-1322, July 2006.